NRL Report 7374

Crack-Growth Resistance Characteristics of High-Strength Sheet Alloys

C.N. Freed, A.M. Sullivan and J. Stoop
Fracture Mechanisms Section
Strength of Metals Branch
Metallurgy Division

January 31, 1972

Security Classification

DOCUMENT CONTROL DATA - R & D

(Security classification of title, body of abstract and indexing annotation must be entered when the overall report is classified)

1. ORIGINATING ACTIVITY (Corporate author)	2a. REPORT SECURITY CLASSIFICATION
Naval Research Laboratory Washington, D. C. 20390	Unclassified
	2b. GROUP

3. REPORT TITLE

CRACK-GROWTH RESISTANCE CHARACTERISTICS OF HIGH-STRENGTH SHEET ALLOYS

4. DESCRIPTIVE NOTES (Type of report and inclusive dates) A final report on one phase of the problem; work is continuing on other aspects.

5. AUTHOR(S) (First name, middle initial, last name)

C. N. Freed, A. M. Sullivan, and J. Stoop

6. REPORT DATE	7a. TOTAL NO. OF PAGES	7b. NO. OF REFS
January 31, 1972	22	8

8a. CONTRACT OR GRANT NO.	9a. ORIGINATOR'S REPORT NUMBER(S)
NRL Problem No. M01-24 b. PROJECT NO. Project RR 022-01-46-5431 c. d.	NRL Report 7374 9b. OTHER REPORT NO(S) (Any other numbers that may be assigned this report)

10. DISTRIBUTION STATEMENT

Approved for public release; distribution unlimited.

11. SUPPLEMENTARY NOTES	12. SPONSORING MILITARY ACTIVITY
	Department of the Navy (Office of Naval Research) Arlington, Virginia 22217

13. ABSTRACT

Crack propagation in a metal sheet is impeded by the inherent resistance to fracture of the alloy. This resistance is manifested by the requirement that crack growth will occur only under a rising load up to an instability load at which unstable fracture commences. If the fracture resistance curve which designates the load-crack extension relationship to instability has a unique shape for each material and is independent of most specimen dimensions, it can be a valuable tool in failure-safe design.

The fracture resistance curves (R-curves) have been obtained for six high-strength sheet alloys which fractured under elastic loads. The influence of three specimen geometric variables and yield strength on the shape of the R-curve and the critical stress-intensity factor K_c was investigated. On several alloys a comparison was made between the R-curve and K_c value generated with a center-cracked tension (CCT) specimen and data derived from a crack-line loaded (CLL) specimen used at Armco Steel Corporation.

The radius of the slit tips in the CCT specimen did not affect the K_c value for aluminum 7075-T6 in which stable crack growth preceded instability. The R-curves emanating from fatigue-cracked specimens did indicate longer crack growth at lower loads than was evident from the blunter slit tips. Both K_c and R curves were generally independent of initial slit length $2a_0$ for aluminum alloys, although some scatter was observed for one steel and the titanium alloy.

The K_c value was independent of specimen width W for high-strength aluminum alloys. The shape of the R-curve for the different CCT specimen widths of 2024-T3 was identical. The inverse relationship between K_c and yield strength was obvious for the aluminum alloys and for 4130 steel.

A comparison of K_c values for the CCT specimen and the CLL specimen indicated some differences for alloys which manifest crack growth under constant load. Since the commencement of constant-load crack growth marks the end of structural integrity, its recognition is crucial to a rational interpretation of

(Continued) —

DD FORM 1 NOV 65 1473 (PAGE 1)

S/N 0101-807-6801

Security Classification

14. KEY WORDS	LINK A		LINK B		LINK C	
	ROLE	WT	ROLE	WT	ROLE	WT
Crack growth resistance curve R-curve Plane stress Elastic-plastic fracture Stress intensity Linear-elastic fracture mechanics Fracture Mechanics Center-cracked tension specimen						

fracture resistance. This behavior is observable on the CCT specimen test record, and the K value at initiation of constant load crack growth is designated as K_c. Because the behavior was not directly observed on the CLL specimen test record, the K_c criterion applied to these specimens was different. Thus, the differences between the K_c values reported by CCT and CLL specimens are attributable to interpretation of data and not to the different methods of load application employed by the specimens.

CONTENTS

ABSTRACT

Crack propagation in a metal sheet is impeded by the inherent resistance to fracture of the alloy. This resistance is manifested by the requirement that crack growth will occur only under a rising load up to an instability load at which unstable fracture commences. If the fracture resistance curve which designates the load-crack extension relationship to instability has a unique shape for each material and is independent of most specimen dimensions, it can be a valuable tool in failure-safe design.

The fracture resistance curves (R-curves) have been obtained for six high-strength sheet alloys which fractured under elastic loads. The influence of three specimen geometric variables and yield strength on the shape of the R-curve and the critical stress-intensity factor K_c was investigated. On several alloys a comparison was made between the R-curve and K_c value generated with a center-cracked tension (CCT) specimen and data derived from a crack-line loaded (CLL) used at Armco Steel Corporation.

The radius of the slit tips in the CCT specimen did not affect the K_c value for aluminum 7075-T6 in which stable crack growth preceded instability. The R-curves emanating from fatigue-cracked specimens did indicate longer crack growth at lower loads than was evident from the blunter slit tips. Both K_c and R curves were generally independent of initial slit length $2a_0$ for aluminum alloys, although some scatter was observed for one steel and the titanium alloy.

The K_c value was independent of specimen width W for high-strength aluminum alloys. The shape of the R-curve for the different CCT specimen widths of 2024-T3 was identical. The inverse relationship between K_c and yield strength was obvious for the aluminum alloys and for 4130 steel.

A comparison of K_c values for the CCT specimen and the CLL specimen indicated some differences for alloys which manifest crack growth under constant load. Since the commencement of constant-load crack growth marks the end of structural integrity, its recognition is crucial to a rational interpretation of fracture resistance. This behavior is observable on the CCT specimen test record, and the K value at initiation of constant load crack growth is designated as K_c. Because the behavior was not directly observed on the CLL specimen test record, the K_c criterion applied to these specimens was different. Thus, the differences between the K_c values reported by CCT and CLL specimens are attributable to interpretation of data and not to the different methods of load application employed by the specimens.

PROBLEM STATUS

This report completes one phase of the problem. Work on other aspects of the problem is continuing.

AUTHORIZATION

NRL Problem M01-24
Project RR 022-01-46-5431

Manuscript submitted November 29, 1971.

CRACK-GROWTH RESISTANCE CHARACTERISTICS OF HIGH-STRENGTH SHEET ALLOYS

INTRODUCTION

The design process for high-performance structures requires the selection of metal properties criteria which will characterize the performance of the material. Conventional design practice which puts inordinately heavy emphasis on tensile test parameters is insufficient for fully rational design. Without consideration of static and dynamic fracture resistance, stress-corrosion sensitivity, and fatigue characteristics, design adequacy cannot be assured.

The fracture resistance of a material is among the most important material properties to be defined. The degradation of the capability of a metal to tolerate flaws as the metal strength is increased is a fundamental problem for the designer who views the use of high-strength alloys as a means to increase structural efficiency. The ability to characterize the fracture resistance properties of high-strength sheet metals permits the effective utilization of the precise structural analysis with which the designer can describe the stress and strain concentrations in the structure.

When high-strength sheet alloys are fabricated, the structure will inevitably contain flaws and cracks which will impair its load-bearing capability. The degree of impairment can be measured by application of the basic parameters of linear-elastic fracture mechanics which defines fracture resistance in terms of the load and crack length relationship required for commencement of unstable crack extension.

FRACTURE RESISTANCE (R) CURVE

The R-curve concept, first promulgated in 1960 (1), suggests that a unique relationship exists between the crack-growth resistance R and the amount of crack extension δa. This relationship describes the crack-growth resistance of a metal alloy. In a rising-load test, the crack-extension force $\mathcal{J}$ increases and is opposed by a resistance to crack extension R. Equilibrium is maintained so that $\mathcal{J} = R$ up to the point of instability, whereupon the driving force overwhelms the capability of the metal to resist crack extension and unstable fracture commences.

An operational definition of instability recognizes that load is not the independent variable in fracture toughness testing; rather it is the separation of the heads of the testing machine, equivalent to overall specimen extension, e. At instability, $dP/de = 0$. Subsidiary test variables are the stress σ and crack length a.

In a quasi-two-dimensional prototype specimen, an appropriate expression for $\mathcal{J}$ is:

$$E\mathcal{J} = \pi\sigma^2 a \quad \text{(Ref. 2)} \qquad (1)$$

Now since $\mathcal{J} = R = 0$, so also does $d(\mathcal{J} - R) = 0$.

Including the subsidiary variables, one obtains

$$d(\mathcal{J} - R/de = \left(\frac{\partial \mathcal{J}}{\partial \sigma}\right)\left(\frac{d\sigma}{de}\right) + \left(\frac{\partial \mathcal{J}}{\partial a}\right)\left(\frac{da}{de}\right) \tag{2}$$

$$-\left(\frac{\partial R}{d\sigma}\right)\left(\frac{d\sigma}{de}\right) - \left(\frac{\partial R}{da}\right)\left(\frac{da}{de}\right) = 0. \tag{3}$$

Since $(d\sigma/de) = 0$ at instability, by definition, this reduces to

$$\left(\frac{\partial \mathcal{J}}{\partial a}\right)_{\sigma = \sigma_c} = \left(\frac{\partial R}{\partial a}\right)_{\sigma = \sigma_c} = 0, \tag{4}$$

where σ_c is the instability or critical value.

If the crack resistance curve, hereafter referred to as the R-curve, has a unique shape for each material and is independent of initial crack length, specimen geometry, and boundary loading conditions, it can be considered a fracture-toughness signature of the metal. A geometry-independent R-curve can be a useful tool to engineers engaged in failure-safe design. Through the use of a numerical solution, the designer can ascertain the tangency point between the crack driving-force curve and the R-curve, and therefore compute the stress intensity at the commencement of unstable crack propagation. Since the equation which describes the crack driving-force curve will approximate the stress distribution and boundary loading conditions of the structure, the tangency point will provide the critical stress vs crack length relationship applicable to the structure at the onset of brittle fracture. Catastrophic failure can be prevented by using a structure design which will keep any stress vs crack length relationship that may occur in service from approaching the critical relationship.

MATERIALS

The fracture toughness of six structural sheet metals was investigated: three aluminum alloys, one titanium alloy, and two steels. All of the sheet was 0.063 in. thick with the exception of the PH 15-7 air melt stainless steel (0.052 in.) and 7475-T61 aluminum (0.090 in.). The mechanical property data and the heat treatments are presented in Table 1.

EXPERIMENTAL PROCEDURE

The R-curve concept has recently been revived to examine its usefulness in defining the fracture resistance of thin sheet metals subject to a plane-stress condition. Heyer and McCabe (3) have utilized the crack-line loaded (CLL) specimen to provide R-curves for a spectrum of metal alloys. A wedge-opening device is used to load the CLL specimen and propagate the crack. Because of the specimen configuration and loading system, the crack never becomes unstable and full R-curves can be developed.

Table 1
Mechanical Properties

Material	Alloy	Fracture Direction	Yield Strength σ_{ys} at 0.2% Offset (ksi)	Ultimate Tensile Strength (ksi)	Elongation %	Heat Treatment
Aluminum	7075-T6	WR	76.5	88.5	11.0	
	7475-T61	WR	59.3	70.4	12.5	
	2024-T3	WR	50.0	69.8	17.0	
Steel	4130	WR	169.5	193.0	3.8	Austenize: 1575°F, 1hr. water spray Temper: 700°F, 30 min., air cool
	4130	WR	178.4	226.1	5.2	Austenize: 1575°F 30 min. water spray Temper: 500°F, 30 min., air cool
	15-7 PH*	WR	212.0	—	—	Heat: 1750°F, 10 min Cool: Air cool to room temp. Cool to -100°F, 8 hrs. Reheat: 1050°F, 1hr.
	15-7 PH*	RW	219.1	229.4	5.2	
Titanium	6A1-4V	WR	151.1	156.3	1.0	Solution anneal: 1700°F, 20 min., water spray Age: 975°F, 8 hrs., Air cool

*Donated and heat treated by Armco Research Laboratory.

The center-cracked tension (CCT) specimen is used at NRL to measure K_c, as this specimen is representative of a structural prototype element. The R-curves were drawn from load and crack-opening displacement data obtained from the K_c investigation.

The plane-stress fracture toughness specimen is presented in Fig. 1. In the center of the specimen a cracklike slit has been introduced and within the slit has been placed a beam displacement gage instrumented with a 4-strain-gage circuit. Upon loading, the borders of the slit are displaced and cracks will initiate at the slit tips along a plane perpendicular to the applied stress. The displacement gage will monitor the crack-opening displacement (COD) via an electrical readout to an X-Y recorder; a previous calibration between COD and crack length enables calculation of crack length at any load level during the test (4). Stable crack growth occurs from each slit tip until the total crack reaches a critical length for the applied stress, whereupon unstable crack propagation ensues and the specimen fractures. The crack length and stress at the onset of instability are used to calculate K_c.

The center slit in the CCT specimen was produced by an electric discharge (elox) method. The root radius of the slit tip was typically 3 to 5 mils, which could be decreased to 1 mil by a second elox operation with a fine electrode. Some specimens were also fatigued to assess the influence of slit-tip sharpness on K_c and the R-curve. When stable crack growth preceded fracture, earlier work has shown the crack to be sufficiently acute to eliminate crack or slit-tip radius as a variable (5).

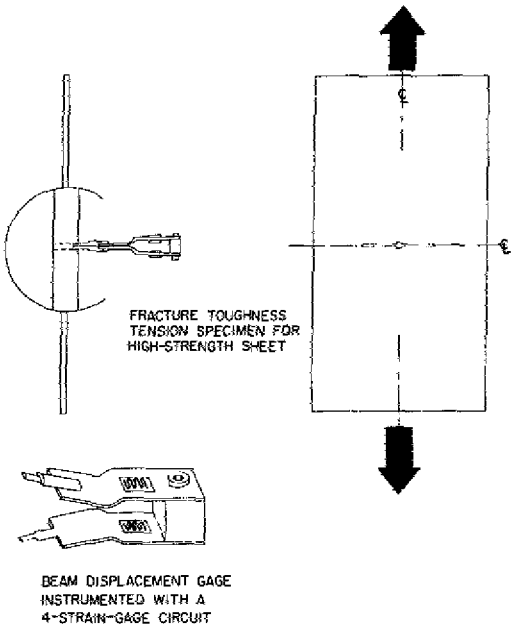

Fig. 1 — Center-cracked tension (CCT) specimen and instrumented beam displacement gage

Specimen width W varied between 12 and 20 in. The length of the unheat-treated specimen was 36 to 40 in. The restricted size of the heat-treating equipment required the use of foreshortened specimens, the length of which was limited to 12 to 15 in. To achieve the desired total testing length, extension tabs were fastened to these specimens with bolts. Previous K_c tests on foreshortened aluminum specimens that were lengthened by extension tabs have demonstrated K_c was unaffected by this technique (4). The PH 15-7 specimens were heat treated at Armco, and the foreshortening method did not have to be employed.

DISCUSSION OF R-CURVES

Aluminum 7075-T6

The fracture toughness properties for Aluminum 7075-T6 and subsequent materials are reported in Table 2. Two lots of this alloy were tested: lot 1 represents sheet stored for a number of years, whereas lot 2 sheet was newly acquired.

In Fig. 2a, R-curve data points are displayed which represent a spectrum of eloxed initial crack lengths $2a_0$ for the CCT specimen. An average curve has been drawn through the cluster of points, as the slight scatter militates against distinction of the individual curves. The data points marked with C indicate the point on the individual curves at which K_c was calculated.

The R-curve appears to be independent of initial crack length for CCT specimens of this alloy. A comparison of the average CCT R-curve with the Armco CLL specimen R-curve for the same alloy indicates that the CLL specimens demonstrated considerably longer crack growth to achieve the same K_R value. The X on the Armco curve at 63.0 ksi$\sqrt{\text{in.}}$ designates the stress-intensity value taken as K_c. This compares well with the average NRL K_c value of 65.2 ksi$\sqrt{\text{in.}}$ for lot 1 computed by averaging more than 20 tests of the CCT specimens containing different initial crack lengths.

Table 2
Fracture Toughness Properties

Material	Alloy	Fracture Direction	Yield Strength (ksi)	Lot No. Specimen	Slit Tip	Specimen Width (In.)	Specimen Geometry	
							CCT K_c (ksi$\sqrt{in.}$)	CLL K_c (ksi$\sqrt{in.}$)
Aluminum	7075-T6	WR	76.5	Lot 1	Elox	12	65.2	—
	7075-T6	WR	76.5	Lot 2	Elox	12	61.2	—
	7075-T6	WR	76.5	Lot 2	Elox-sharp	12	61.0	—
	7075-T6	WR	76.5	Lot 2	Elox-fatigue crack	12	59.0	63.0
	7475-T61	WR	59.3	—	Elox	12	88.4	118.1
	2024-T3	WR	50.0	—	Elox	12	97.2	86.0
						15	97.2	—
						20	102.7	106.0
Steel	4130	WR	169.5	—	Elox	12	160.0	—
	4130	WR	178.4	—	Elox	12	140.8	—
	15-7 PH	WR	212.0	—	Elox	11	117.8	90.0
	15-7 PH	WR	212.0	—	Elox	12	109.8	—
	15-7 PH	WR	212.0	—	Elox	20	137.6	90.0
	15-7 PH	RW	219.1	—	Elox	5	222.0	—
	15-7 PH	RW	219.1	—	Elox	10	243.3	—
	15-7 PH	RW	219.1	—	Elox	12	258.5	
	15-7 PH	RW	219.1	—	Elox	20	294.2	—
Titanium	6A1-4V	WR	151.1	—	Elox		74.4	—
	6A1-4V	WR	151.1	—	Elox-fatigue crack		86.1	—

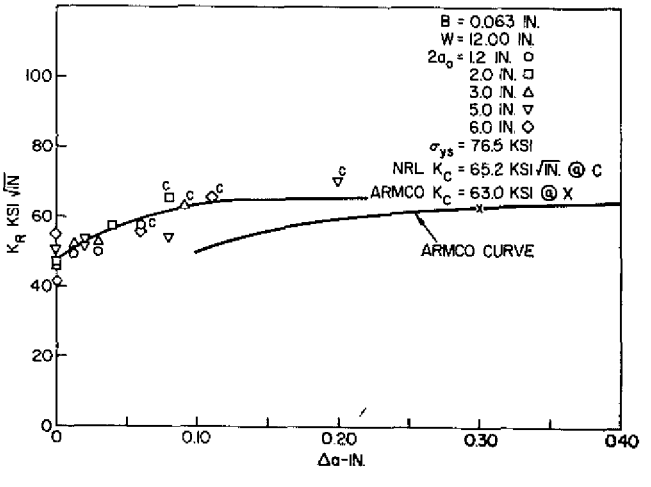

Fig. 2a — Crack-growth resistance K_R for aluminum alloy 7075-T6 plotted as a function of crack growth $\Delta a = a - a_0$. K_c indicated by C for CCT specimens, and by X for CLL specimens (Armco). Radius of the slit tips was 0.003 to 0.005 in.

To understand the influence of the initial slit tip radius on K_c and the R-curve, the original eloxed slits which had an average slit tip radius of 0.004 in. were re-eloxed with a very thin electrode. The sharp elox slits which extended the original slits were 0.002 in. wide, 0.05 in. long, and contained an average radius of 0.001 in. The slit tip radius was further reduced by fatiguing a crack at the tip of the sharp elox slits. The R-curves for the sharp slits of lot 2 are presented in Fig. 2b and for the fatigued specimens in Fig. 2c.

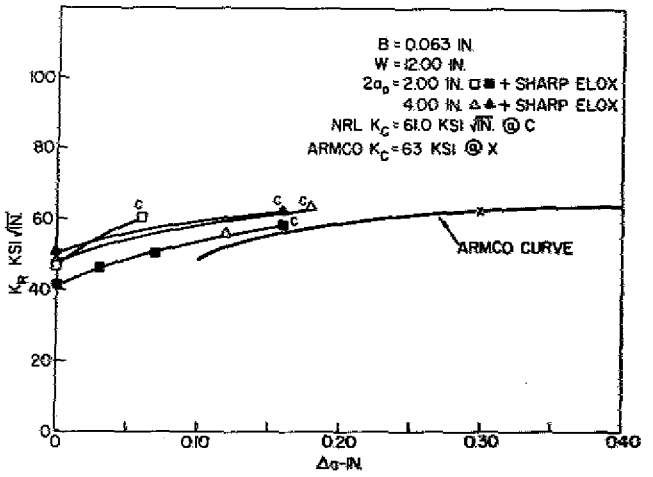

Fig. 2b — As Fig. 2a; slit tips extended by a sharp elox slit (0.06 in. long, .002 in. wide) tip radius of about 0.001 in. Amount of crack growth similar to that in Fig. 2a.

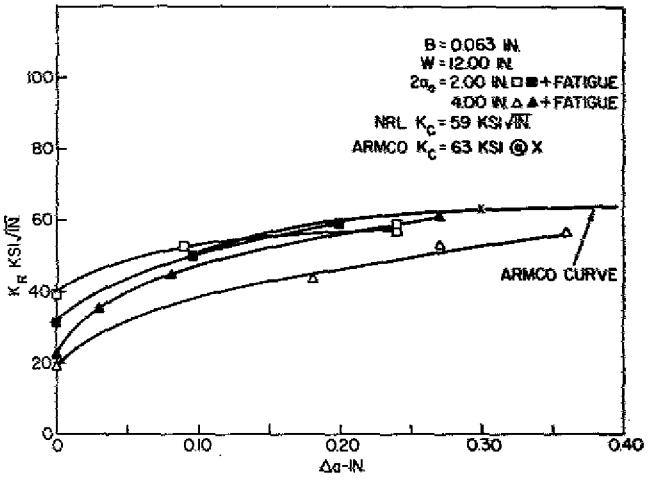

Fig. 2c — As Fig. 2a; slit tips extended by a fatigue crack. Amount of crack growth prior to instability has increased to that of CLL specimen.

The sharp slit R-curves (Fig. 2b) demonstrate slightly greater crack growth before failure than did the curves for the single elox operation of Fig. 2a, although the Armco curve continues to exhibit longer crack extension. The R-curves representing the fatigued specimens of Fig. 2c show considerable crack growth and overlap the Armco R-curve with the exception of one curve which fell low. The average K_c values for these lot 2 materials of 61 ksi$\sqrt{in.}$ for the sharp eloxed specimens and 59 ksi$\sqrt{in.}$ for fatigue-cracked specimens are commensurate with unpublished data on lot 2 material using the blunter elox slit in which K_c = 61 ksi$\sqrt{in.}$

Aluminum 7475-T61

The data for this tougher aluminum alloy are shown in Fig. 3. The CCT curves for $2a_0$ of 2- and 3-in. eloxed slits appear identical to each other and to the Armco CLL data. The K_c values obtained by the different specimens are, however, significantly different: the CCT values average 88 ksi$\sqrt{in.}$, whereas, the CLL specimen evidenced a toughness of 118 ksi$\sqrt{in.}$ The difference is believed to be a result of the dependency of crack growth behavior on specimen design and is discussed in more detail in another section of this report.

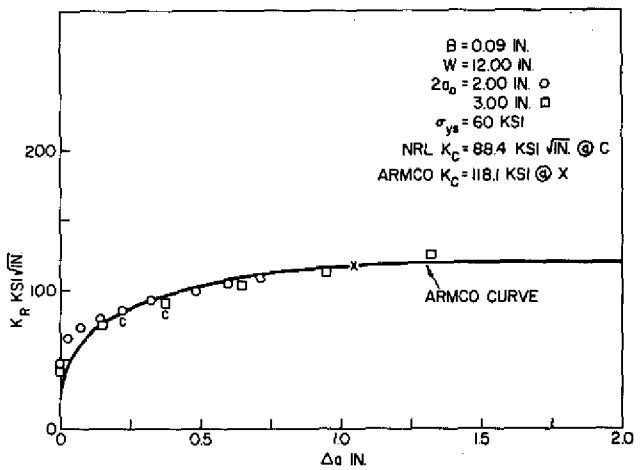

Fig. 3 — Crack growth resistance K_R for aluminum alloy 7475-T61 WR plotted as a function of Δa. Instability value of K_c indicated by "C" for CCT specimens by "X" for CLL specimens. Armco (CLL) curve fits CCT specimen R-curve but K_c values differ.

Aluminum 2024-T3

R-curve data points for 12-in.-wide CCT specimens of 2024-T3 are plotted in Fig. 4a, and for 20-in.-wide specimens in Fig. 4b. The Armco curve represents an average of two CLL specimen geometries 2T and 4T, 5- and 10-in. widths, respectively.

Close agreement exists between the shape of the R-curves for the CCT and CLL specimens with the CCT specimens manifesting a slightly higher K value throughout the range of crack extension. Initial crack length did not influence K_c for the CCT specimens

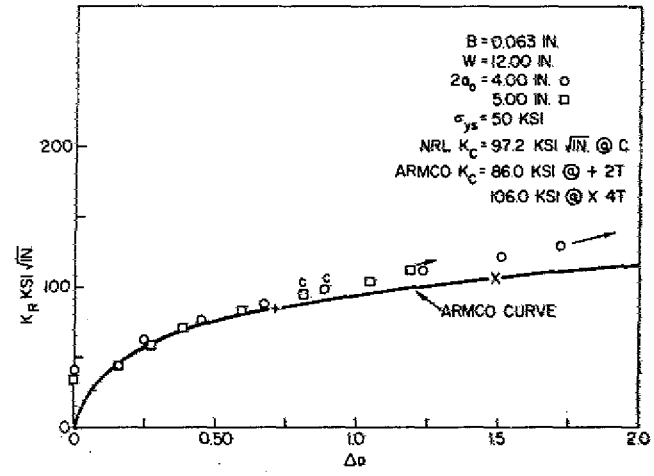

Fig. 4a — Crack growth resistance K_R for aluminum alloy 2024-T3, direction WR. Instability value of K_c indicated by "C" for 12-in. wide CCT specimen, and "X" for CLL specimen. Arrows indicate crack growth beyond limit of CCT calibration curve. R-curves from both specimen geometries are close fitting but K_c values differ.

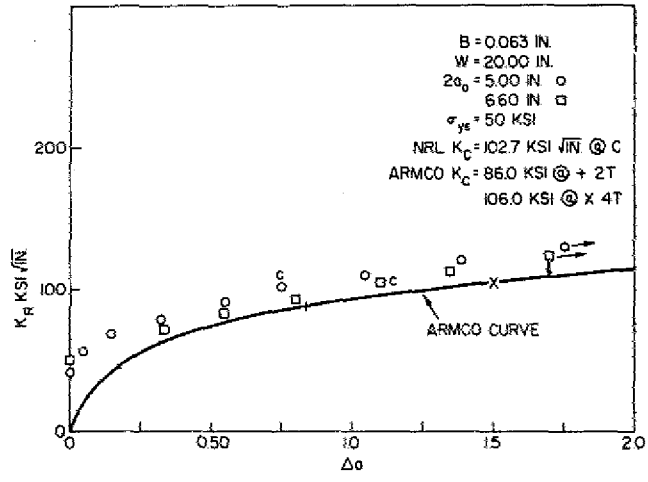

Fig. 4b — As Fig. 4a but width W = 20 in. Although Armco curve is slightly low, it is probably within normal scatter range.

of either the 12- or 20-in. width. The Armco data do indicate the possibility of an effect of CLL specimen width on K_c; the K_c of the 2T specimen (5 in. wide, but considered equivalent to a 10-in.-wide CCT specimen) is 86 ksi$\sqrt{\text{in.}}$, whereas the 4T specimen (10 in. wide, equivalent to a 20-in.-wide CCT specimen) measured K_c = 106 ksi$\sqrt{\text{in.}}$ The slight difference between K_c values for the two widths of the NRL data indicates that if CCT specimen width has an influence on K_c the effect is slight.

Steel PH 15-7

The PH 15-7 stainless steel sheet employed in this investigation was donated by Armco in the heat-treated condition. Several CCT specimen widths were used and an R-curve comparison for the WR and RW fracture direction is presented in Figs. 5a and 5b, respectively.

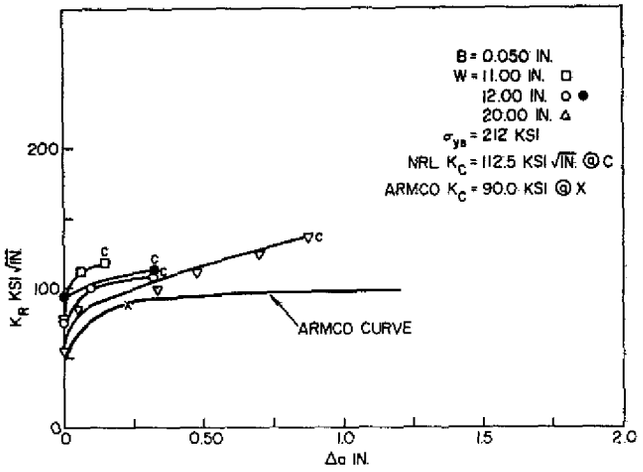

Fig. 5a — Crack growth resistance K_R for stainless steel PH 15-7 (air melt), direction WR. Instability value of K_c indicated by C for CCT specimen and by X for CLL specimen. Inexplicably high K_c value noted for 20-in.-wide CCT specimen.

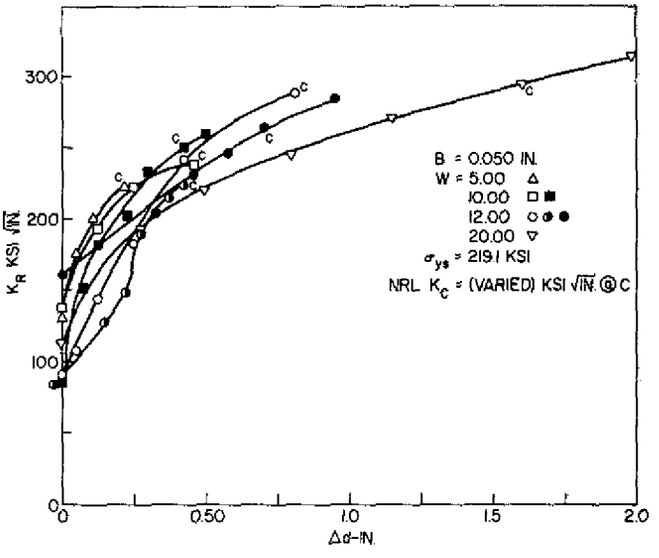

Fig. 5b — As Fig. 5a; direction RW. Note influence of specimen width on the R-curve for this high-toughness fracture direction as reflected by board K_c scatter.

As evidenced by Fig. 5a, both the CCT specimen R-curves and the instability points for the WR fracture direction fell significantly above the CLL curve established with 2T and 4T specimens. The CCT R-curves can be distinguished according to specimen width with the narrower specimen lying further from the Armco curve. Considerable scatter was also evidenced for the R-curves generated by testing the material in the RW fracture direction. Again, the width effect could be roughly discerned, with the wider CCT specimen producing the generally lower R-curve. The K_c values were spread over such a broad range that no characteristic value is quoted for the RW fracture direction. Center-cracked tension specimens wider than 20 in. must be tested before the RW fracture resistance of this tough material can be ascertained.

Steel 4130

This steel alloy sheet was heat treated to two yield strength levels of 169.5 and 178.4 ksi. CCT specimens containing a range of initial crack lengths were investigated to determine K and to establish R-curve data. The results of this study are displayed in Figs. 6a and 6b.

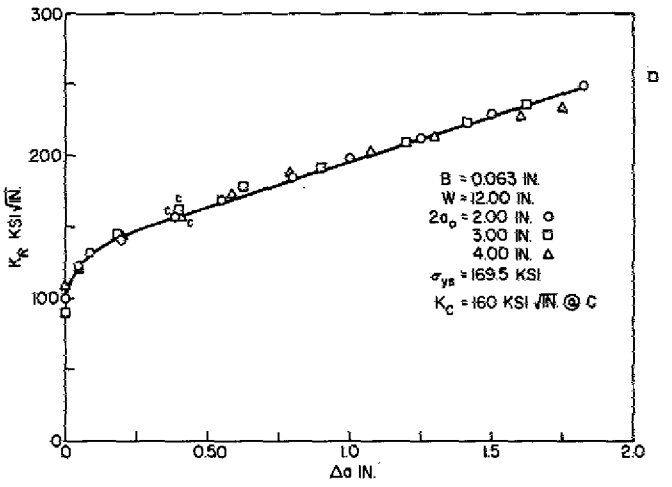

Fig. 6a — Crack growth resistance K_R for 4130 steel, σ_{ys} = 169.5 ksi. Instability values of K_c indicated by C.

When the slit length was varied between 2 and 4 in., the fracture toughness of the lower strength sheet was independent of the initial length of the eloxed slit $2a_0$. This is evident in Fig. 6a in which the R-curves and instability values for different $2a_0$ are indistinguishable. Scatter was present in the higher strength sheet of Fig. 6b, but a trend was not discernible. There are no CLL specimen data available for this alloy.

Titanium Ti-6Al-4V

Center-cracked tension specimens of heat-treated 6Al-4V titanium sheet were investigated over a range of initial slit lengths and the results are presented in Fig. 7. There seems to be a tendency, previously observed in aluminum alloys, for specimens with the longer $2a_0$ values to manifest more crack growth than specimens with shorter initial slits.

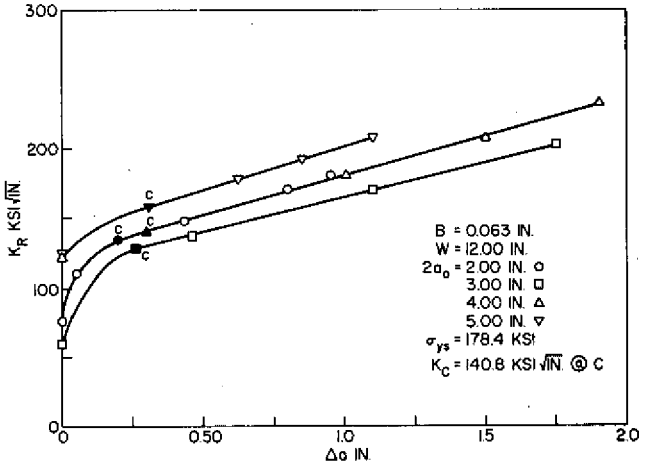

Fig. 6b — As Fig. 6a; σ_{ys} = 178.4 ksi.

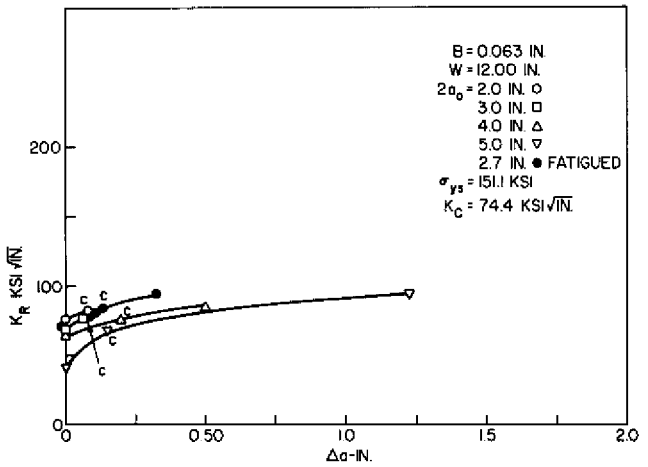

Fig. 7 — Crack growth resistance for titanium alloy 6Al-4V. Instability values of K_c indicated by C.

R-curve shape and K_c values are also distinguishable according to initial slit length although the K_c range is narrow.

Two distinct types of fracture behavior were observed and are commented upon later in this report. The one fatigue-precracked specimen exhibits no increase in crack growth prior to instability. There is no CLL specimen data with which the CCT specimen results may be compared.

DISCUSSION OF EXPERIMENTAL DATA

An examination of the load-crack growth record has revealed several types of crack extension behavior and these are schematically illustrated in Fig. 8. Region I defines the load required to initiate crack growth at the slit or fatigue crack tip. Once formed, the crack will commence stable growth under a rising load (Region II) and if the load is held

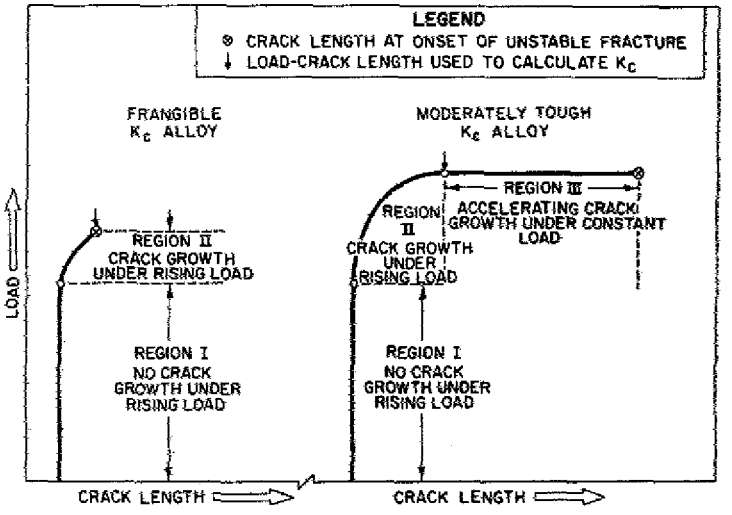

Fig. 8 — Schematic of two types of crack extension behavior, one in which final separation occurs at some value of the rising load, and the other in which final separation occurs after a period of crack growth under a constant load.

constant, the crack will arrest within this region. For the more brittle alloys, once the crack has grown to a critical length, stable growth will give way to unstable fracture.

While the tougher alloys share Region I and II behavior with the more brittle alloys, fracture does not occur under a rising load. Instead, after the crack has slowly extended under a rising load, the crack growth rate will begin to accelerate while the load on the specimen remains constant. Fracture of the specimen quickly follows. For practical purposes the beginning of Region III where the crack begins to grow at constant load marks the limit of structural integrity as failure of the structure is assured. Therefore, the crack length at the commencement of Region III is used to calculate K_c.

Data for σ_G vs 2a are presented from which the previously discussed R curves were obtained. In addition, crack growth curves calculated from the CLL specimen R-curve data are included. This calculation can be accomplished for any assumed crack length 2a and width W by adding values of Δa to a_0 and calculating first 2a/W and finally σ_G from the relationship

$$\sigma_G = \frac{K(\text{at } \Delta a)}{\sqrt{a}\ (2a/W)}.$$

Aluminum 7075-T6

The crack growth curves for 7075-T6 are presented in Fig. 9. The hyperbole curve intersecting each of the CCT specimen crack growth curves represents the average K_c value of 65 ksi$\sqrt{\text{in.}}$ for this alloy. The straight line drawn diagonally across the figure designates the locus of points on which the net stress is equal to the yield stress; any point on the crack growth curve lying to the left of the line denotes a net stress less than the yield stress. The closed data points on the CLL (Armco) specimen curves mark the stress and crack length used to calculate K_c.

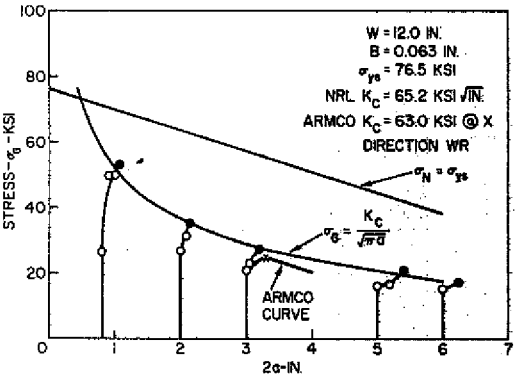

Fig. 9 — Gross stress σ_G (equivalent to load) plotted against crack length 2a for aluminum alloy 7075-T6. Note that instability occurred under rising load in NRL curves and well-defined maximum load in constructed Armco curve. Instability location marked by solid symbols.

Both the redrawn CLL curve and the CCT specimen curves rise to a maximum load without encountering constant-load crack growth (Region III behavior). The CLL K_c value of 63 ksi$\sqrt{in.}$ closely corresponds to K_c = 65 ksi$\sqrt{in.}$ for the CCT specimens.

Aluminum 7475-T61

For this tougher aluminum alloy, both the CCT and CLL specimens demonstrate crack growth at constant load (Fig. 10). The K_c value of 118 ksi$\sqrt{in.}$ reported for the CLL specimen was calculated from a crack length equivalent to the end of the constant-load crack growth region; at the commencement of Region III, K_c = 105 ksi$\sqrt{in.}$ for this specimen. The CCT specimen data produce an average K_c = 88 ksi$\sqrt{in.}$ calculated at the beginning of Region III while another laboratory using the CCT specimens reports K_c = 85 ksi$\sqrt{in.}$ (6). It should also be noted that the CLL specimen loaded in tension develops a value of K_c = 111 ksi$\sqrt{in.}$ and shows no region of crack growth under constant load (7).

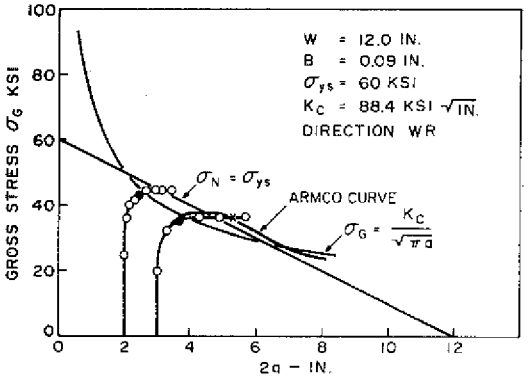

Fig. 10 — Gross stress σ_G plotted against crack length 2a for aluminum alloy 7475-T61. Note region of crack growth under constant gross stress (equivalent to constant load) and similar region in constructed Armco curve. Instability location marked by solid symbols.

Aluminum 2024-T3

As indicated in Fig. 11a and 11b, the crack growth curves for both the redrawn CLL data and the CCT data rise to a maximum stress and remain essentially constant for a long period of crack growth. The instability point for the CLL curve is at the beginning of Region III in Fig. 11a but occurs after considerable constant-load crack growth has taken place for the wider specimen (4T) of Fig. 11b. The K_c values for the 12-in.-wide CCT

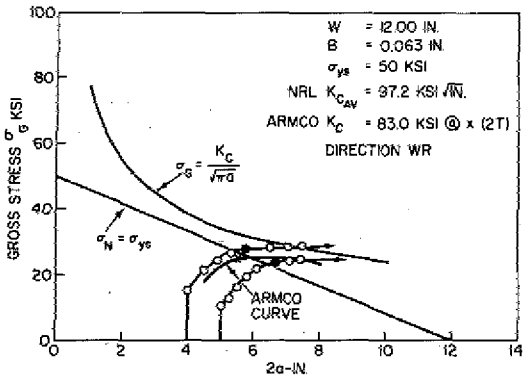

Fig. 11a — Gross stress σ_G plotted against crack length 2a for aluminum alloy 2024-T3 (specimen width 12 in.). Note region of crack growth under constant stress and similar region in constructed Armco curve. Instability location marked by solid symbols. Although the CCT specimen at instability manifested $\sigma_N > \sigma_{ys}$, a K_c value compatible with that from the wider specimen was obtained.

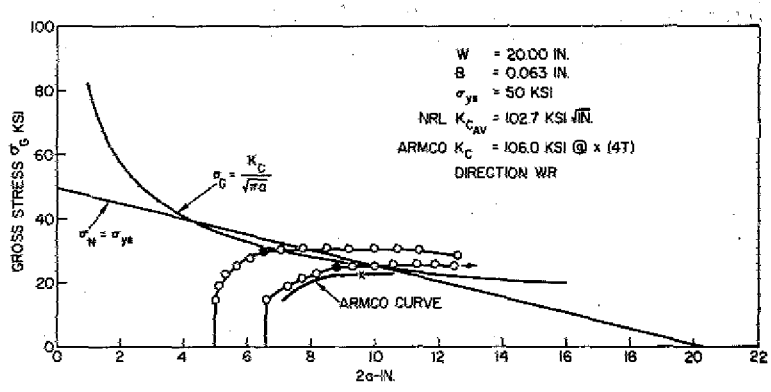

Fig. 11b — As Fig. 11a but W = 20 in. At instability, $\sigma_N < \sigma_{ys}$.

specimens (K_c = 97 ksi$\sqrt{in.}$) are calculated from stress values which just exceeded the yield stress but closely corresponded in K_c values from the 20-in.-wide CCT specimens (K_c = 102 ksi$\sqrt{in.}$) for which instability preceded the yield stress.

Steel PH 15-7 and 4130

Little indication of crack extension at constant load is seen for the PH 15-7 stainless steel specimens (Fig. 12) for either CCT or CLL specimen geometry except for the 20-in.-wide CCT specimen in the RW direction (not shown).

The crack growth curve for 4130 steel CCT specimens is plotted in Figs. 13a and 13b. In each case the crack growth was stress dependent until a stress level was attained at which the crack extended at constant load culminating in fracture after 1 to 3 in. of crack extension. Region III behavior was common to specimens of both yield strength levels.

Titanium Ti-6Al-4V

The crack growth characteristics for this alloy are plotted in Fig. 14. All of the specimens displayed sufficient crack extension prior to fracture to obviate the possibility

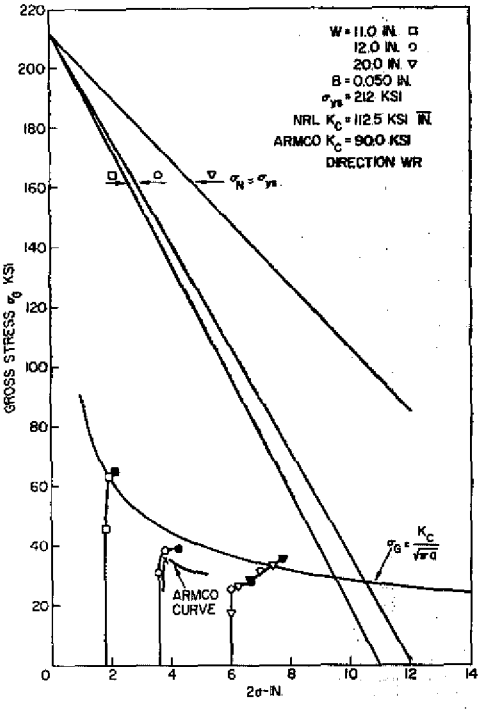

Fig. 12 — Gross stress σ_G plotted against crack length 2a for stainless steel PH 15-7 (air melt), direction WR. Similar to Fig. 9, the curve shows that crack growth to instability occurs under rising load only and is reflected in well-defined maximum of Armco curve. Apparent shape of 20-in.-wide specimen curve is somewhat abnormal and may indicate an experimental anomaly. Instability location marked by solid symbols.

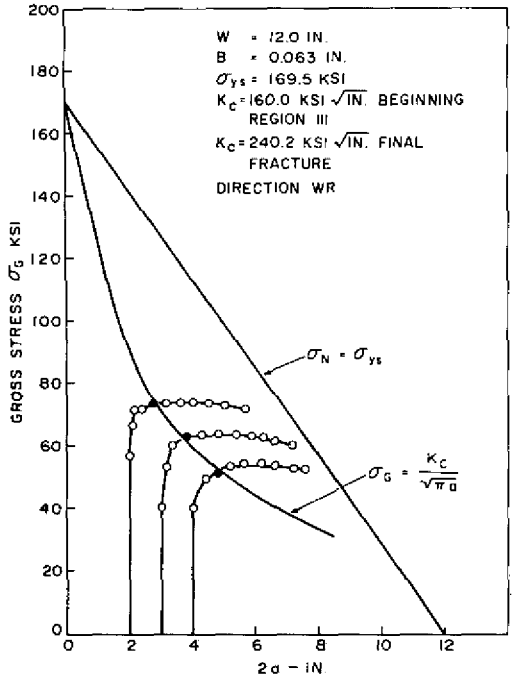

Fig. 13a — Gross stress σ_G plotted against crack length 2a for 4130 steel (σ_{ys} = 169.5 ksi). Region of crack growth under constant load terminates in final separation before yield stress is reached in specimen net section. Instability location marked by solid symbols.

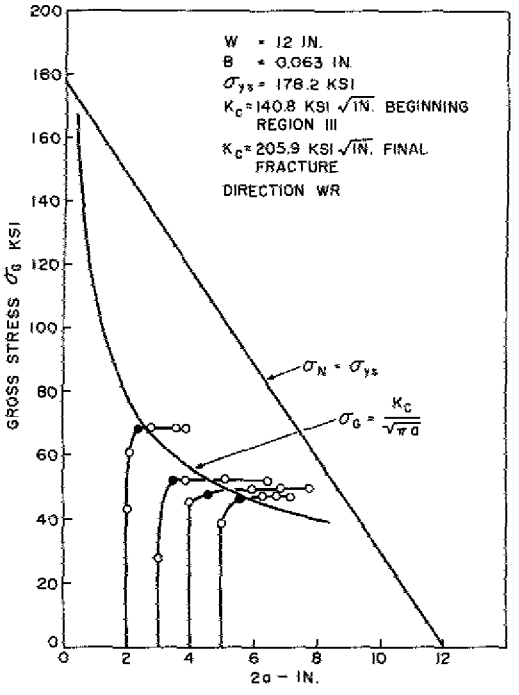

Fig. 13b — As in Fig. 13a; σ_{ys} = 178.4 ksi.

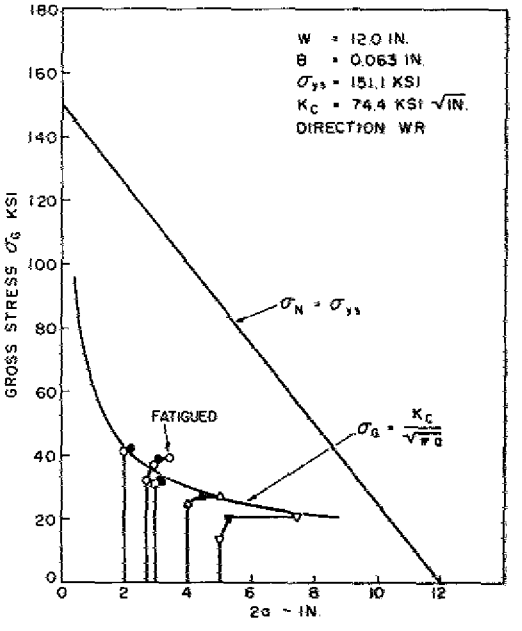

Fig. 14 — Gross stress σ_G plotted against crack length 2a for titanium alloy 6Al-4V. Instability location marked by solid symbols. Note here both types of crack extension behavior.

that recorded K_c values were affected by the crack tip radius. The CCT specimens containing the shorter initial slits did not demonstrate Region III behavior, whereas those specimens with the longer $2a_0$ did evidence constant-load crack growth.

It should be noted that the constant K_c hyperbolic curve drawn in each of these figures was based on the infinite sheet formula, whereas the instability points for each specimen were calculated with the Isida finite width equation (8). This accounts for the deviation between the mean value of the instability points and the position of the constant-K_c

curve. It should also be noted that for some materials, instability and final separation occurred at net stress values below general yield, showing that Region III behavior is not a phenomenon associated with general yield in the specimen.

These data illustrate the types of response to loading which can be expected of sheet metal containing notches or cracks. To the designer, once the crack begins to propagate under a constant load or stress, structural integrity has been lost. Therefore, the K_c value separating Region II from Region III is considered to represent the effective fracture resistance of the material. This value does not appear to be indicated by the CLL specimen.

SUMMARY

The effect of slit tip radius on K_c was investigated for 7075-T6 sheet of 1/16-in. thickness. No significant change in K_c was observed over a slit tip radius varying from 0.005 in. to fatigue crack sharpness. As stable crack growth preceded instability, it would be expected that K_c would be independent of the acuity of the slit tip. An opposite and probably anomalous effect was noticed for Ti-6Al-4V. Recent results indicate that when instability occurs immediately upon reaching maximum load without prior crack extension, the slit tip radius may have to be considered.

Although no influence of the slit tip radius on K_c for 7075-T6 was recorded, the tip sharpness did affect the shape of the crack extension R-curve. While the R curves of both eloxed slits and sharp eloxed slits were similar, the crack extension curves from slit tips extended by fatigue cracks exhibited longer crack growth at lower loads prior to instability. The latter curves closely resembled the R-curves obtained with CLL specimens.

The relationship between specimen width and K_c appears to be straightforward for aluminum alloys. For 2024-T3, K_c is not a function of width for $W \geq 12$-in. The 12-in.-wide specimens were the equivalent of 20 times the plane-stress plastic zone radius† r_y. Earlier work on 7075-T6 had demonstrated that if $W > 26r_y$, valid K_c values could be obtained. The results of the width study of PH 15-7 stainless steel are indecisive. The 11-in.-wide WR specimen was the equivalent of $W = 22.5r_y$, and by the aluminum criteria should have been sufficiently wide. Yet the K_c value of the 20-in.-wide stainless was significantly higher than either the 11- or 12-in.-wide specimens. It is presently unclear why a width dependence was observed for this alloy.

The K_c- and R-curves were generally independent of initial slit length $2a_0$ for the aluminum alloys over the range of slit lengths investigated. Some scatter was observed for one of the strength levels of 4130 and Ti-6Al-4V but no discernible trend was in evidence. The inverse relationship between K_c and yield strength was obvious for the aluminum alloys and for 4130 steel.

In a structure, failure is imminent once a crack starts to propagate under constant load. For that reason, when crack growth at constant load was observed in a CCT test, the K value at the commencement of this behavior was deemed the effective fracture toughness of the sheet. Mathematical tangents to R-curves produced either by the CLL or

---

† $r_y = \frac{1}{2\pi}\left(\frac{K_c}{\sigma_{ys}}\right)^2$.

the CCT specimen are not sufficiently discriminatory to identify the onset of constant-load crack extension; it must be checked by data and/or plots of gross stress σ_G vs crack length. The advantage of the CCT specimen is that the initiation of this behavior is readily identifiable even from raw data, whereas a conversion computation must be made for the CLL specimen data to change $K_R - a$ to a $\sigma_G - 2a$ curve.

REFERENCES

1. Krafft, J. M., Sullivan, A. M., and Boyle, R. W., "Effect of Dimensions on Fast Fracture Instability of Notched Sheets," Proc., Crack Propagation Symposium, College of Aeronautics, Cranfield, England, 1961, Vol. I, pp. 8-28 (published 1962).
2. Srawley, J. E., and Brown, W. F., Jr., "Fracture Toughness Testing Methods," *Fracture Toughness Testing and Its Applications*, ASTM STP 381, 133-196, 1965, Discussion, pp. 196-198.
3. Heyer, R. H., and McCabe, D. E., "Plane Stress Fracture Toughness Testing Using a Crack-Line-Loaded Specimen," *J. Eng. Fracture Mech.* (submitted for publication).
4. Sullivan, A. M., and Freed, C. N., "The Influence of Géometric Variables on K_c Values for Two Thin Sheet Aluminum Alloys," NRL Report 7270, June 17, 1971.
5. Broek, D., "The Residual Strength of Aluminium Sheet Alloy Specimens Containing Fatigue Cracks or Saw Cuts," National Aerospace Laboratory (Amsterdam) Technical Report NLR-TR M. 2143, March 1966.
6. Alcoa Aerospace Technical Information Bulletin, Series 71, No. 6, 1971, Pittsburgh, Pa.
7. Heyer, R. H., and McCabe, D. E., "Test Method — Fracture Toughness Measured, by Crack Growth Resistance," Armco: Research and Technology Report, Middletown, Ohio, Jan. 27, 1971.
8. Brown, W. F., Jr., and Srawley, J. E., "Plane Strain Crack Toughness Testing of High Strength Metallic Materials," ASTM STP 410, American Society for Testing and Material, Philadelphia, Pa., 1966.